



Daniela Barras Nunes Serra e Silva

Bachelor of Science in Materials Engineering

Additive fabrication of 3D anepectic structures

Dissertation to obtain the Master's Degree in
Materials Engineering

Supervisor: Professor Doutor Alexandre Velhinho, Professor Auxiliar, Faculdade de Ciências de Tecnologia da Universidade Nova de Lisboa

Co-supervisor: Professor Doutor João Paulo Borges, Professor Auxiliar, Faculdade de Ciências e Tecnologias da Universidade Nova de Lisboa

Jury:

Chairperson: Doutor Rui Jorge Cordeiro Silva, Professor Associado com Agregação do Departamento de Ciências dos Materiais da NOVA School of Science and Technology | FCT NOVA

Raporteurs: Doutor João Paulo Heitor Godinho Canejo, Investigador do Departamento de Ciências dos Materiais da NOVA School of Science and Technology | FCT NOVA

Members: Doutor Alexandre José da Costa Velhinho, Professor Auxiliar do Departamento de Ciências dos Materiais da NOVA School of Science and Technology | FCT NOVA

Additive Fabrication of 3D Aneptic Structures

Copyright © Daniela Barras Nunes Serra e Silva, Faculty of Sciences and Technology, NOVA University of Lisbon. The Faculty of Sciences and Technology and the NOVA University of Lisbon have the right, perpetual and without geographical boundaries, to file and publish this dissertation through printed copies reproduced on paper or on digital form, or by any other means known or that may be invented, and to disseminate through scientific repositories and admit its copying and distribution for non-commercial, educational or research purposes, as long as credit is given to the author and editor.

“The wonderful arrangement and harmony of the cosmos would only originate in the plan of an almighty omniscient being. This is and remains my greatest comprehension.”

Sir Isaac Newton

ACKNOWLEDGMENTS

Em primeiro lugar, gostaria de agradecer aos meus orientadores, Professor Doutor Alexandre Velhinho e Professor Doutor João Borges, por toda a disponibilidade, paciência e orientação ao longo dum trabalho bastante interessante e desafiante (especialmente em tempos de pandemia), no qual estou bastante grata pela oportunidade em participar.

Também gostaria de agradecer a toda a equipa do DCM e do CENIMAT, assim como a todos os professores do Departamento de Ciências dos Materiais, pelo apoio indispensável ao longo do meu percurso académico. Em especial, agradeço ao João Cardoso, por toda a ajuda e atenção disponibilizadas ao longo desta dissertação.

Um especial obrigado à minha família. Em particular, aos meus pais por todo o amor, sacrifício e apoio incondicional; agradeço também por me terem transmitido valores preciosos e eternos. Aos meus avós maternos, por todo o amor, atenção e paciência indispensáveis para o meu crescimento.

Por fim, agradeço a Deus pelo sustento constante, amor imerecido e bênçãos incontáveis. É de coração completo a transbordar de gratidão e felicidade que declaro: “... Tu és o meu Senhor; não tenho outro bem para além de ti.” (Salmos 16:2).

ABSTRACT

This work focuses on the design and manufacture (by additive fabrication) of 3D anepectic structures. These anepectic structures have two rare characteristics: they exhibit negative values of Poisson's ratio and of coefficient of thermal expansion (CTE). Negative values of CTE are activated by the combination of two different materials, in which both have positive values of CTE. This type of structure is useful in applications such as in the biomedical and aerospace fields, where it is important to have a mechanical response to a thermal stimulus.

Ten samples were studied and subjected to thermo-mechanical tests: five single material samples (four of Nylon and one of CPE+) and five dual material samples (four of Nylon-PVA and one of Nylon-CPE+). All samples were subjected to tensile tests in which the most negative value of Poisson's Ratio achieved in this work was of -1.103. All samples were subjected to thermal tests, in which they were submerged in silicone oil (Baysilone M350) and, then, subjected to a heating process. In this type of test, the most negative value of CTE was of $-812 \times 10^6 / ^\circ C$ at $120^\circ C$.

Keywords: 3D Printing, Auxetic, Negative Thermal Expansion, Anepectic, Negative Poisson's ratio.

RESUMO

Este trabalho foca-se no desenho e fabricação (por fabricação aditiva) de estruturas anepéticas 3D. Essas estruturas anepéticas possuem duas características raras: apresentam valores negativos de coeficiente de Poisson e de coeficiente de expansão térmica (CET). Valores negativos de CET são ativados pela combinação de dois materiais diferentes, no qual ambos têm valores positivos de CET. Este tipo de estrutura é útil em aplicações como na área biomédica e aeroespacial, onde é importante ter uma resposta mecânica a um estímulo térmico.

Dez amostras foram estudadas e submetidas a testes termo-mecânicos: cinco amostras de um só material (quatro de Nylon e uma de CPE+) e cinco amostras de dois materiais (quatro de Nylon-PVA e uma de Nylon-CPE+). Todas as amostras foram submetidas a ensaios de tração em que o valor mais negativo do coeficiente de Poisson obtido neste trabalho foi de -1.103. Todas as amostras foram submetidas a testes térmicos, em que foram imersas em óleo de silicone (Baysilone M350) e sujeitas a um processo de aquecimento. Neste tipo de teste, o valor mais negativo de CTE foi de $-812 \times 10^{-6}/^{\circ}\text{C}$ a 120°C .

Palavras-chave: Impressão 3D, Auxética, Expansão térmica negativa, Anepética, Coeficiente de Poisson negativo.

LIST OF CONTENT

Acknowledgements	vii
Abstract	ix
Resumo	xi
List of Figures	xv
List of Tables	xvii
Acronyms	xix
Symbols	xxi
1. Introduction	1
1.1 NTE Materials	1
1.2 Auxetic Materials.....	2
1.3 Additive Fabrication.....	3
1.4 Anepeptic Materials.....	3
2. Materials and Methods	5
2.1 Structure Design	5
2.2 Filament characterization and Thermo-mechanical Evaluation of Structures	6
3. Results and Discussion	7
3.1 Materials	7
3.2 Auxetic Behaviour	8
3.3. Values of the coefficient of thermal expansion	9
3.3.1. Effect of material combination	10
3.3.2. Effect of structure architecture and of length	11
3.3.3. Effect of temperature above glass transition temperature	11
4. Conclusions and Future Perspectives	13
References	15
Appendix.....	19

LIST OF FIGURES

Figure 1.1 – Main structures of auxetic structures: a1) Re-entrant Honeycomb [30]; a2) Re-entrant star-shaped [31]; b) Chiral [32]; c) Rotating Units [33].	2
Figure 1.2 – 2-D (I and II), 3-D ((a)-(d)) anepectic structures and their resultant unit cells (e)-(h) designed by Ai and Gao [44].	4
Figure 2.1 – Two main anepectic structures were designed, printed and tested: a) – Structure I: Star Honeycomb Structure; b) – Structure II: Star-shaped re-entrant structure.	5
Figure 3.1 – PR values for all the samples.	8
Figure 3.2 - Photos of the structures tested in this work.	9
Figure 3.3 – CTE of all the structures at 80°C.	10
Figure 3.4 – CTE of structures #1, #1 75%, #2 and #2 75% in the material combination of Nylon-PVA at 80°C.	11
Figure 3.5 – CTE of structure #1 in different material combinations (Nylon, Nylon-PVA and Nylon-CPE+) at different ranges of temperature: 25°C to 40°C, 25°C to 80°C and 25°C to 120°C.	12
Figure A.1 - Representative scheme and description of the testing structure performed in this work.	19
Figure C.1 - Tensile curves of three polymeric materials (Nylon, CPE+ and PVA) used in this work as constituents of the printed structures. The materials used were commercially available Ultimaker™ filaments. The specimens were tractioned (2 mm/min) by using a universal testing machine (AG-50kNG, Shimadzu, Japan).	20
Figure E.1 - Sample Nylon #2 with the circles marked, and the A and B representative positions.	22
Figure F.1 - Figure F.1 – Sample Nylon #2 during tensile tests: a) – Sample Nylon #1 non-deformed; b) – Sample Nylon #1 deformed.	23

LIST OF TABLES

Table 2.1 - Parameters used in structures #1 and #1 75%.	6
Table 2.2 - Parameters used in structures #1 and #1 75%.	6
Table 3.1 – Material properties for Nylon, CPE+ and PVA.	7
Table 3.2 - Summary of structures studied in this work. × not tested. ✓, tested.	8
Table 3.3 – Values of Tg for Nylon, PVA and CPE+[1].	11
Table D.1 - The materials' properties used in this work. All the polymers used are commercially available Ultimaker™ filaments and they were tested to determine their values of CTE, Young's Modulus and glass transition temperature. These values are important to determine which are the best combinations to obtain an anepectic behaviour.	21

ACRONYMS

2-D	Two dimensional
3-D	Three dimensional
4-D	Four dimensional
CPE+	Copolyester +
CTE	Coefficient of thermal expansion
GPa	Gigapascal
NPR	Negative Poisson's ratio
NTE	Negative thermal expansion
PVA	Polyvinyl alcohol

SYMBOLS

α	Coefficient of thermal expansion
H1	Length parameter
H2	Length parameter
L1	Length parameter
L2	Length parameter
min	minute
mm	millimetre
°C	degrees Celsius
s	seconds
t	Length parameter
Tg	Glass transition temperature in °C
θ	Angle parameter
θ_o	Angle parameter
ν	Poisson's Ratio

A metamaterial is an artificially engineered material whose physical properties are influenced by the adjustment of its architecture instead of its composition. This type of material exhibits properties that rarely appear in conventional materials. An anepectic material is a material that demonstrates negative values not only of coefficient of thermal expansion (NTE) but also of Poisson's Ratio (NPR). Considering that, to obtain negative values of Poisson's ratio, the material's geometry must be adjusted in patterns structured with precise shape, geometry, size and orientation [1], it is possible to affirm that the anepectic material is a metamaterial.

This type of metamaterial has a great range of applications such as the biomedical field (fabrication of fillings for dental restorations, stents and surgical hernial meshes), sensors and electronics, aerospace and defence (antennas, solar panels, and sturdier structures) [2], because it can control distortions resultant of vibrations due to thermal changes, which indicates that anepectic materials are an asset for situations where is extremely important to have mechanical stability in thermally unstable conditions.

1.1 NTE Materials

Thermal expansion focuses on the dimensional variation of a material caused by its thermal variation. Most materials tend to expand when heated and to contract when cooled (materials with a positive thermal expansion). However, materials with NTE have the opposite behaviour: they contract when heated and they expand when cooled.

This type of material has several applications such as in satellite antennas, space telescope mirrors, space vehicles (aerospace industry), dentall filling composites (biomedical field) and bridges (civil engineering) [1]. To sum up, NTE materials are useful in environments where there's a temperature disparity (which leads to a thermal stress disparity) and, therefore, it is extremely important to have a precise control of thermal expansion.

However, natural materials with negative thermal expansion are rare and they only manifest it in a narrow range [3]. The small amount of NTE conventional materials is caused by the abnormal mechanisms that must occur to have a negative thermal expansion (ie: phase transitions, shortening of bond lengths, rigid unit modes, electronic effects and magnetostriction). The lack of performance is caused by narrow temperature range of negative thermal expansion, low thermal expansion coefficient value, anisotropy of thermal response and low design freedom. This situation can be found in most NTE natural materials like perovskite, $NaZn_{13}$ - type $La(Fe, Si, Co)_{13}$ compounds, $Ag_3[Co(CN)_6]$, $(Hf, Mg)(WO_4)_3$ and the ZrW_2O_8 family materials [4].

Considering this situation, it is predictable that the interest in obtaining materials with negative values of CTE (coefficient of thermal expansion) that have a better performance has increased. Therefore, several structures of, for example, lattice unit cells have been developed with the objective to embody a NTE metamaterial. For instance, there have been proposed buckling origami structures [5] and spherical structures [3]. In the last decades, there have been efforts to develop several 2-D and 3- D NTE structures [3]-[10]. However, most of NTE metamaterials are in 2-D due to two main causes: limitations in fabricating 3-D structures with highly complex geometric patterns and limited material choices to build NTE structures (which

means that NTE could not be tuned within a pre-selected range of temperatures) [1]. Despite of these limitations, NTE metamaterials are efficient to avoid certain undesired occurrences such as thermal twist, buckling and distortion, thermomechanical failure, and fatigue from thermal stress mismatch; NTE metamaterials are also efficient in maintaining geometric stability [3].

1.2 Auxetic Materials

Poisson's Ratio is the ratio of transverse strain to longitudinal strain under applied loading. It was developed by Siméon Poisson [11], a French mathematician and physicist.

In liquids, Poisson's Ratio is 0.5 while in gas or cork it is close to zero. This situation demonstrates that the volume of a liquid is always constant, but in the case of gas or cork, there's a volume variability. In case of solids such as metals or functional oxides, the Poisson's Ratio is usually 0.1–0.3. For linear elastic isotropic materials, the Poisson's Ratio is confined within the range from -1 to 0.5 [12].

Materials that have positive values of Poisson's Ratio tend to contract in the transverse direction when tensioned in the longitudinal direction and vice-versa. Materials with NPR (auxetic materials) have the opposite response: they tend to expand in the transverse direction when tensioned in the longitudinal direction. This type of material (auxetic) appears in different structures, materials and scales (macro- or micro-scales) and it can be considered a metamaterial, regarding that it's an artificially engineered material.

Auxetic materials have been deeply used in the biomedical field for the fabrication of bioprostheses (annuloplasty prostheses, cushion pads and knee prosthetics). At a cellular level, there have been developments in biological scaffolds (creation of suspended web structures that exhibit positive and negative values of Poisson's ratio) and hydrogels that contain two different types of pores in which their size, shape and distribution can alter Poisson's ratio from positive to negative at micro-scale [13]. This type of material stands out for having certain mechanical characteristics significantly improved such as shear resistance, indentation resistance, fracture toughness [12], energy absorption [11], ability to create cellular structures with shape memory (in other words, shape memory auxetic) and variable permeability [13].

The term "auxetic" has a Greek origin: $\alpha\upsilon\tilde{\xi}\eta\tau\iota\kappa\acute{o}\varsigma$ (auxetikos), that means "which tends to increase". This word first appeared in a paper by Evans et al. in 1991 [14]. However, the term "auxetic" appears later than the first research related to the concept of Negative Poisson's Ratio made by Lakes [15] in 1987.

Despite of considering an auxetic material a metamaterial, there are some natural materials that have an auxetic behaviour. The first natural material to be discovered with this characteristic was iron pyrite by Love [16]. Later, other auxetic materials were also discovered such as cancellous bone, living cat skin and cow teat skin [17].

Over the past 30 years, there has been a great progress in this field. It has been studied the auxetic behaviour in cellular structures (in micro- or macro-scale) [18]-[28]. Several 2-D and 3-D auxetic materials with different structures were designed and analyzed such as: re-entrant (honeycomb [21], [24], [29],[30] and star-shaped [31]); chiral models ([32]); rotating units [28], [33]. Additive fabrication is one of the techniques most used to manufacture auxetic metamaterials (ie: [34]-[36]).

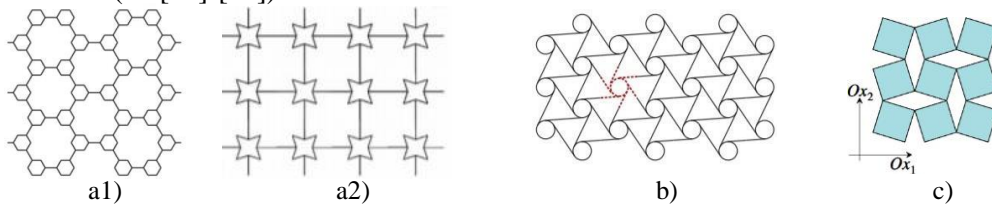


Figure 1.1 – Main structures of auxetic structures: a1) Re-entrant Honeycomb [30]; a2) Re-entrant star-

shaped [31]; b) Chiral [32]; c) Rotating Units [33].

More recently, there have been developments in 4-D auxetic printed structures (the fourth dimension refers to time). This means that 4-D printed materials are responsive materials that change their configuration over time, due to an external stimulus [2]. To embody 4-D printed auxetic materials, there have been used several types of materials like functional polymers, magneto—rheological fluid suspensions and shape memory alloys. However, Shape-Memory Polymers (SMPs) are the most studied in this matter; these type of materials exhibit SME (Shape-Memory Effect): the ability to return from a deformed temporary shape to the original permanent shape through the application of a thermal stimulus [37]. It is important to note that additive fabrication has taken great importance in the manufacture of 4-D auxetic materials.

1.3 Additive Fabrication

Additive fabrication – it can also be called additive manufacturing (AM) or 3-D printing – is a technique in which materials are deposited in layers in order to produce a structure and it has the capacity to produce complex geometries. This type of technique can fabricate a full object or to finish an object's fabrication from a semi-finished part and it is applicable to a wide range of materials (ie: metals, polymers, ceramics, composites).

This recent technique, compared with the other traditional manufacturing techniques, has three main advantages: freeform fabrication (there aren't any traditional manufacturing restrictions and, therefore, provides design freedom); short supply chain (reduction of supply chain of fabrication and maximization of profit space for manufacturers); sustainable manufacturing (reduction of the environmental impact) [38].

The first technological approach to additive manufacturing was made by Charles Hull in 1984 who introduced the Stereolithography technique. Since then, great developments have been occurred in this area and nowadays, there are several types of additive fabrication. For instance, one of the most used AM technologies are extrusion deposition processes in which there are three main processes: fused deposition modelling (FDM), fused filament fabrication and melt extrusion manufacturing (MEM) [39]. Additive fabrication is, nowadays, a technology that has several applications such as biomaterials [40], defence [41] and aerospace [42]. However, this technique is still recent, and it is expected that many other developments and applications about this topic will come to light in the next few years.

1.4 Anepeptic Materials

The term “anepeptic” comes from the Greek *Επέκταση* (*Epéktasi*) that means “Expansion” for materials that have NTE and NPR. However, this term is far more recent than most papers about this type of material: it is first mentioned in literature in a paper by J.Raminhos *et al* [1].

Regarding that an anepeptic material is a metamaterial, it is foreseeable that all the investigation about it gives great importance to its design. For instance, a paper by Joseph N. Grima *et al* [43] proposes a connected triangles structure (rotating triangles connected by pin joints). Other paper by Ai and Gao about 2-D lattice-based metamaterials [44] proposes the combination of an auxetic structure and a bi-material lattice design to achieve a 2-D anepeptic material. Later, Ai and Gao extended their previous work by designing a 3-D anepeptic material [45].

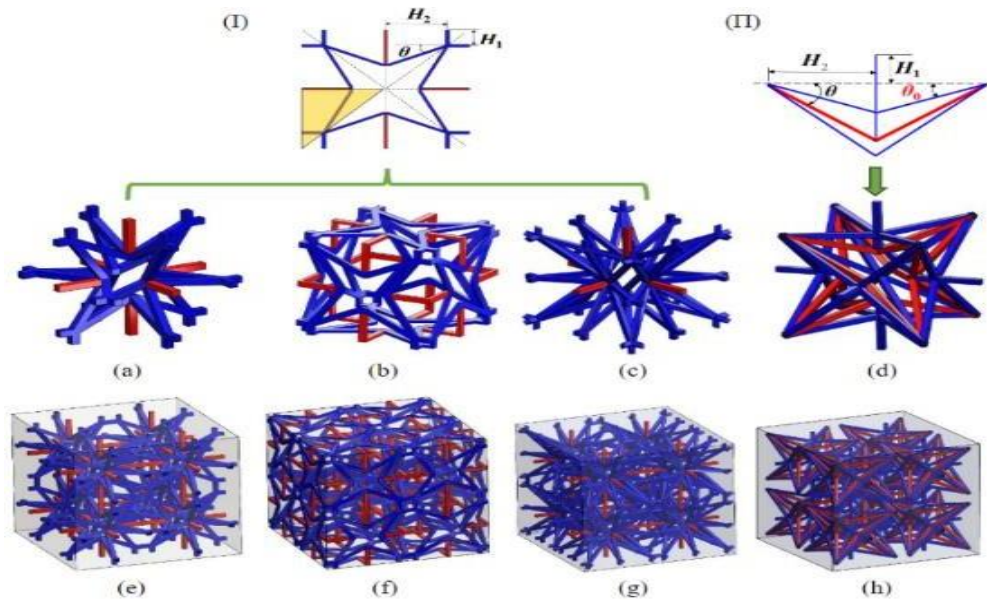


Figure 1.2 – 2-D (I and II), 3-D ((a)-(d)) anepectic structures and their resultant unit cells (e)-(h)) designed by Ai and Gao [44].

However, these papers mentioned didn't managed to embody the anepectic material that was, so far, just a theoretical matter. The first non-virtual 2-D anepectic mesh was achieved by J.Raminhos *et al* [1]; in that work, a polymer-based composite mesh was manufactured by additive fabrication. Later, 2-D anepectic composite meshes, made from ABS and NiTi alloys, were fabricated by an additive manufacturing technique (Fused Filament Technique) and characterized [2]. Other recent paper about this topic focuses on design and additive fabrication of 2-D composite anepectic meshes with incorporated wires that can induce a controlled temperature through resistive heating by applying electric current [13].

To sum up, the combination of two different materials in an auxetic structure causes the activation of the NTE behaviour and, therefore, leads to anepectic behaviour. However, as mentioned by J.Raminhos *et al* [1], it is also important to fulfil this condition: the materials used must have similar (although different) stiffness but extremely different values of CTE and they must work above their respective transition glass temperature (T_g).

Anepectic materials are expected to have several applications such as in the dental field (fillings), the aerospace industry (antennas, solar panels, sturdier structures) and in the biomedical field (stents and surgical hernial meshes) [2].

This work focuses on two main star-shaped re-entrant structures. The following sections explain how these structures were designed and subjected to thermal and mechanical tests (determination of the values of CTE and of the Poisson's ratio); it is also explained how the filaments used in this work were characterized.

2.1 Structure Design

This work is an extension of the work developed by J.Raminhos *et al* [1] in which a new challenge is proposed: to manufacture non-virtual 3- D anepectic structures.

The anepectic material is obtained by combining an inherently auxetic structure with a dual-material NTE structure design. In this work, two main structures are studied, as shown in Figure 2.1. Both belong to the category of re-entrant in shape of star structures. One of them is a star honeycomb structure (based on one of the structures designed by M.S.Ra *et al* [46]). The other structure – based on the structure shown in Figure 1.2 d) - refers to a star-shaped re-entrant structure (the term “re-entrant” refers to a negative angle or an angle greater than 180 degrees [11]). Despite of their design differences, both structures have a similar mechanism: when stretched, their cells tend to open, causing auxetic effect.

In this work, the blue beams represent the material with the lowest CTE, but with the higher stiffness while the red beams represent the material with the much higher CTE, but with the slightly lower stiffness. When all the needs to achieve an anepectic behaviour are fulfilled, the resultant structure in Figure 1.3-a) has three length parameters (L_1 , L_2 and t) and one angle parameter – θ . The resultant structure in Figure 2.1-b) has five geometrical parameters: H_1 , H_2 , θ and θ_o (shown in Figure 1.2 d)) and t (shown in Figure 2.1 b)) in which three of them (H_1 , H_2 and t) are length parameters and the other two (θ and θ_o) are considered angle parameters. In this work, 3-D anepectic structures will be designed, fabricated and tested (determination of their thermal and mechanical behaviour). To manufacture the desired structures, a commercially available 3-D printer will be used and there won't be any pins, adhesives, welding or pressure-fit joints involved.

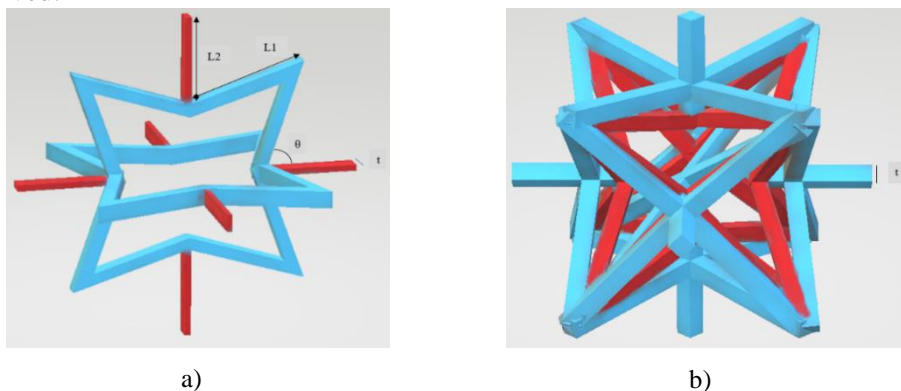


Figure 2.1 – Two main anepectic structures were designed, printed and tested: a) – Structure I: Star honeycomb structure; b) – Structure II: Star-shaped re-entrant structure.

To design the intended structures, it was used the modeling software *123D Design*. The structures were printed by *Ultimaker 3TM* fused filament 3-D printing-system by *Ultimaker* that

can process two different materials simultaneously. All the materials used in this work are commercially available *Ultimaker 3TM* filaments. To ensure good quality printing, the abovementioned structures were printed with support - it was developed by the 3-D printing software *Ultimaker Cura*.

In this work, four structures are designed are printed. Two of them are the main structures (structures #1 and #2) and the other two are the secondary structures (structures #1 75% and #2 75%) in which their thickness was reduced about in 25%. Structures #1 and #1 75% have dimensions of 60.6 mm×60.5 mm× 60.5 mm. Structures #2 and #2 75% have dimensions of 65.5 mm×63.5 mm×64.3 mm. All the structures were printed with a 95% infill density (which means that they are solid structures) and with a layer thickness of 0.2mm.

With the objective to have an auxetic behaviour, structures #1 and #1 75% have a crucial condition to fulfil: $\theta > \frac{\pi}{4}$. Structures #2 and #2 75% also have some conditions to maintain their auxetic behaviour: $\theta_0 < \theta$; $0 \leq \theta \leq 45^\circ$.

Table 2.1 – Parameters used in structures #1 and #1 75%.

Parameters	L1 (mm)	L2 (mm)	θ ($^\circ$)	t (mm)
Structure #1	22.0	16.6	72.4	3.1
Structure #1 75%	22.0	16.6	72.4	2.3

Table 2.2 – Parameters used in structures #2 and #2 75%.

Parameters	H1 (mm)	H2 (mm)	θ ($^\circ$)	θ_0 ($^\circ$)	t (mm)
Structure #2	9.5	28.4	15.6	6.3	3.3
Structure #2 75%	9.5	28.4	15.6	6.3	2.5

2.2 Filament characterization and Thermo-mechanical Evaluation of Structures

In this work, the abovementioned structures were subjected to thermo-mechanical tests. All the materials used to embody these structures are commercially available *Ultimaker 3TM* polymer filaments.

First, it was tested the mechanical capabilities of the structures. Single and dual material structures (#1, #1 75%, #2, #2 75%) were tested (their dimensions and values of length parameters are explicit above). Tensile strength was applied, in which different samples suffered a constant elongation rate of 2 mm/min up to 5 mm overall elongation. It was used an universal testing machine (AG-50kNG, Shimadzu, Japan) whose load cell was of 500 N. These tensile tests were useful to determine two important parameters in this work: Young’s Modulus and Poisson’s ratio. Each sample was monitored using a digital camera that recorded the entire testing process. To determine the values of those two parameters, the resultant images of these tests were analysed by the image processing software *ImageJ*.

Then, it was tested the thermal behaviour of the structures (CTE values), in which it was used a transparent container with silicone oil (Baysilone M350). In this type of test, the structures were held to a wire (that was suspend to a tripod) and, then, they were submerged in the silicone oil. After that, the structures were stabilized for 10 minutes. Next, the silicone oil was heated at a rate of 3°C/min, until the temperature of 80°C was reached. Each tested sample was monitored using a digital camera: photographs were taken at a rate of 1 photograph/°C. The temperature of the silicone oil was monitored by an external thermocouple and data logger (Pico TC-08 with a Type K thermocouple).

The representative scheme and description of the testing structure, equations (of PR and CTE) and the procedures to determine experimental values of PR and CTE can be found in the Appendix.

As already mentioned, anepectic structures have two main characteristics – exhibition of negative values of coefficient of thermal expansion and of Poisson’s Ratio. In this chapter, the following sections will approach these topics: the choice of materials that will embody the designed structures and the thermo-mechanical tests’ results – these data are highly important to verify if the structures designed and printed have all the requirements needed to obtain an anepectic behaviour.

3.1 Materials

In Chapter 1, it was mentioned that, to have an anepectic behaviour, it is important to have a dual-structure design in which the chosen materials have similar stiffness and largely different values of CTE.

Therefore, there were chosen two types of combinations - Nylon-PVA and Nylon-CPE+ - since these combinations fulfil the abovementioned requirement. However, it is expected that the pair Nylon-CPE+ will have a worse performance for two reasons: the pair Nylon-CPE+ has more similarity in stiffness than the pair Nylon-PVA (the chosen materials must have similar stiffness, but not too similar: comparing pairs with similar stiffness, the pair with higher disparity in stiffness is more desirable) and also the pair Nylon-CPE+ has less disparity in values of CTE in which, in this case, is more desirable to have the highest disparity of CTE possible. To sum up, it is possible to conclude that both the pairs are recommended, however, the pair Nylon-PVA is a more ideal combination, as Table 3.1 shows.

Table 3.1 – Material properties for Nylon, CPE+ and PVA.

Materials	Young’s Modulus (GPa)	CTE ($\times 10^{-6}/^{\circ}\text{C}$)
Nylon	0.907	149
CPE+	1.199	58
PVA	2.365	14

In this work, single and dual material structures were printed. Single material structures were printed with the purpose of confirming, comparing with the dual material structures, that all the structures have an auxetic behaviour, regardless of their material composition. Dual material structures are printed to confirm that the anepectic behaviour depends only of their material combination.

Table 3.2 - Summary of structures studied in this work. × not tested. ✓, tested.

	Material(s)	Structure #1	Structure #1 75%	Structure #2	Structure #2 75%
Dual material structures	Nylon-PVA	✓	✓	✓	✓
	Nylon-CPE+	✓	×	×	×
Single material structures	Nylon	✓	✓	✓	✓
	CPE+	✓	×	×	×

3.2 Auxetic behaviour

As previously mentioned in Chapter 2, single and dual-material structures were tested through tensile mechanical tests to ensure that all the structures have an auxetic behaviour – this behaviour is inherent to their geometry, not to their material combination.

During the tests, the selected structures were subjected to an overall elongation of 5 mm at room temperature, with a constant elongation rate of 2 mm/min.

As it can be seen in Figure 3.1, the tensile tests demonstrate, as expected, that all the structures have an auxetic behaviour, not because of their material combination, but because of their geometry. It is also possible to note that, regardless of the material, structure #1 shows a more exacerbated auxetic behaviour than structure #2 (the geometry of this type of structure is more complex, which makes deformation more difficult). Besides, comparing the thicker structures (#1 and #2) with the thinner structures (#1 75% and #2 75%), it is possible to conclude that less thickness leads to a more auxetic behaviour. These tensile tests also demonstrate that there's a discrepancy between the values of single material structures and dual-material structures. This discrepancy happens, because in the dual-material structures, there's a predominance of the stiffer material (PVA in the structures Nylon-PVA and CPE+ in the structures Nylon-CPE+) which prevents the structures to deform so easily, leading to a less significant auxetic behaviour.

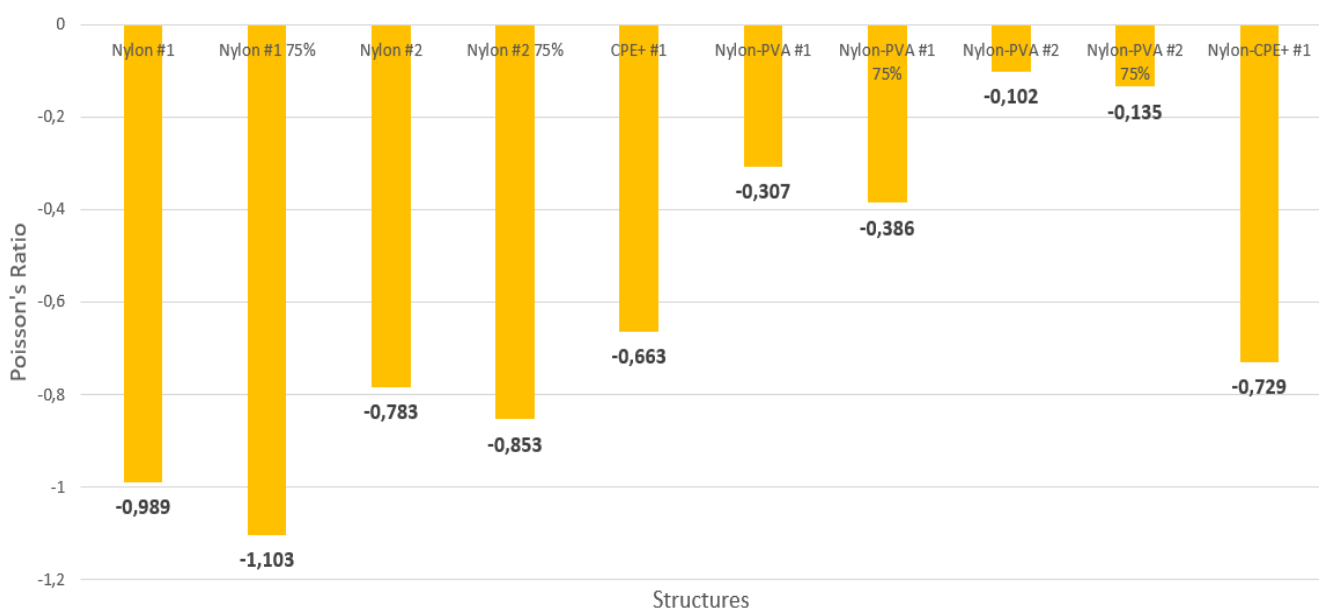


Figure 3.1 – PR values of all the samples.

3.3 Values of the coefficient of thermal expansion

Ten samples were subjected to thermal variation (as it can be seen in Figure 3.2), in which the resulting deformation was consideration.

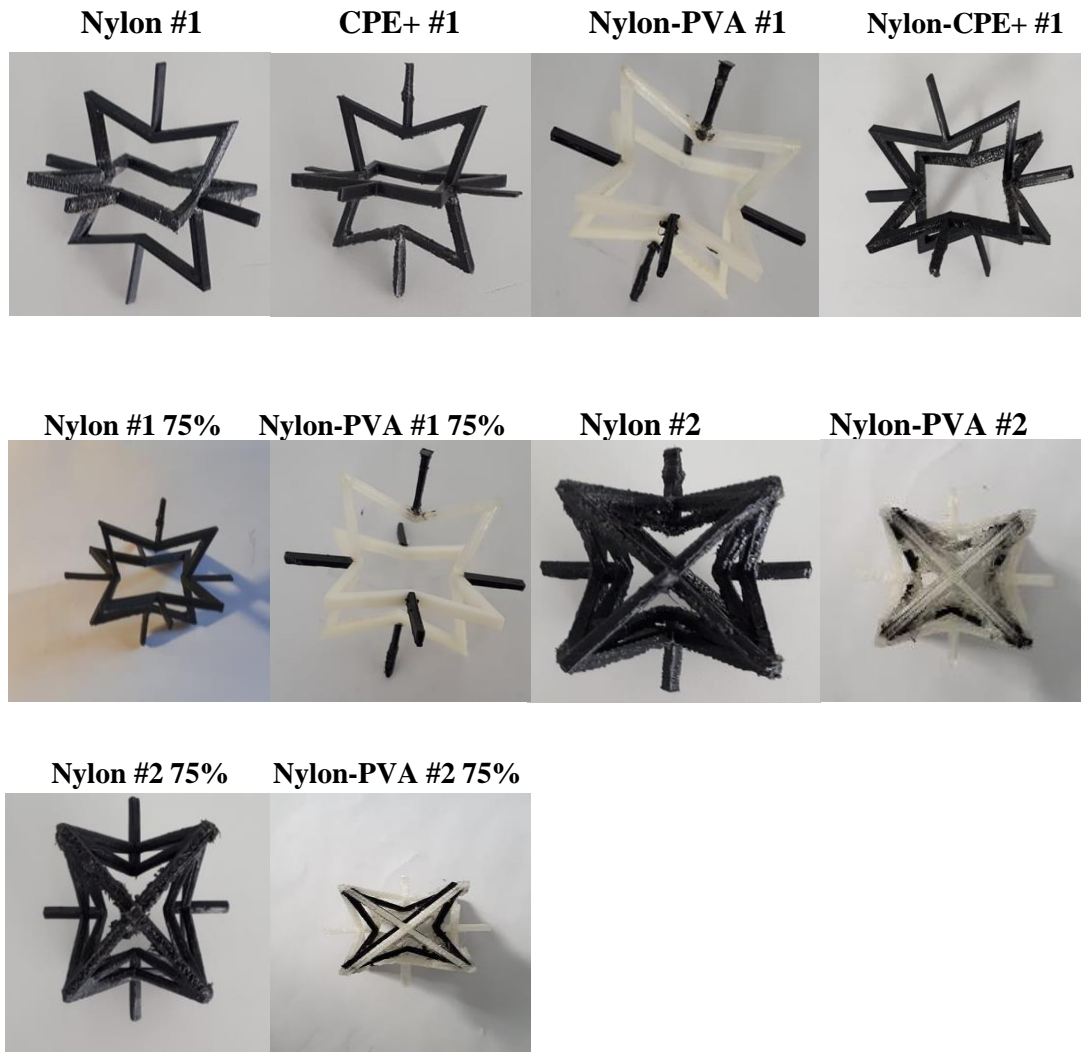


Figure 3.2 Photos of the structures tested in this work.

3.3.1 Effect of material combination

In this work, ten samples (five single material samples and five dual material samples) were thermally tested to demonstrate how the material combination can influence CTE values. All the samples were subjected to heating from room temperature (25°C) to 80°C. As Figure 3.3 shows, dual-material structures (except Nylon-CPE+ #1) are the only structures with NTE behaviour and, therefore, the only structures that have anepectic behaviour.

As expected, according to the data in Figure 3.3, single material structures show positive values of CTE: Nylon #1 ($157 \times 10^{-6}/^{\circ}C$), Nylon #1 75% ($178 \times 10^{-6}/^{\circ}C$), Nylon #2 ($126 \times 10^{-6}/^{\circ}C$), Nylon #2 75% ($134 \times 10^{-6}/^{\circ}C$) and CPE+ #1 ($70 \times 10^{-6}/^{\circ}C$). Nylon-PVA structures show negative values of CTE: Nylon-PVA #1 ($-520 \times 10^{-6}/^{\circ}C$), Nylon-PVA #1 75% ($-712 \times 10^{-6}/^{\circ}C$), Nylon-PVA #2 ($-230 \times 10^{-6}/^{\circ}C$) and Nylon-PVA #2 75% ($-292 \times 10^{-6}/^{\circ}C$). These results confirm that NTE behaviour does not depend of the structures' geometry, but it depends only of the structures' material combination.

However, it is possible to see that the Nylon-CPE+ combination didn't show negative values of CTE ($86 \times 10^{-6}/^{\circ}C$). Considering these data, it is possible to conclude that the Nylon-CPE+ combination isn't a good combination to obtain anepectic behaviour. Nevertheless, it is also important to note that at 80°C, both Nylon and PVA are working above their respective glass transition temperature (T_g). Therefore, it is expectable that Nylon-PVA samples show negative values of CTE. However, CPE+ does not reach glass transition temperature at 80°C (it only reaches it at 105°C). To sum up, to conclude if the Nylon-CPE+ combination is a good combination, it is necessary to observe this sample at higher temperatures.

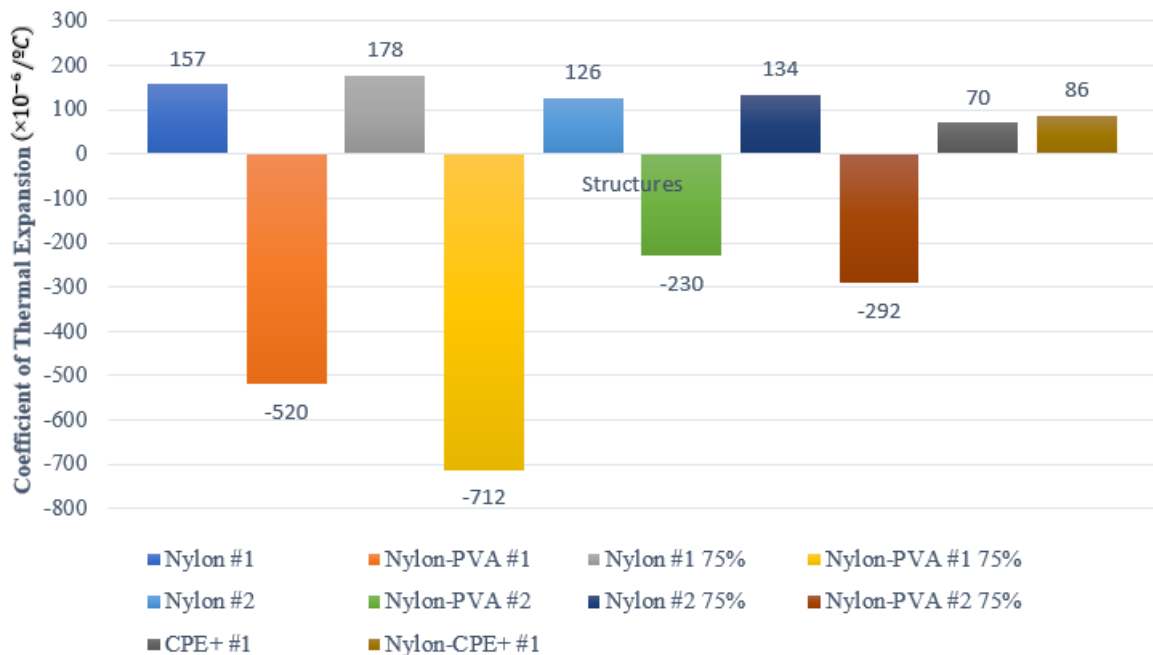


Figure 3.3 – CTE of all the structures at 80°C.

3.3.2 Effect of structure architecture and of length

According to the thermal test described above, it is possible to conclude that the Nylon-PVA combination is a good combination to obtain anepectic behaviour. Nevertheless, it is important to elucidate which is the best geometry and what impact does length have in the anepectic behaviour.

Structures #1 (Nylon-PVA #1 and #1 75%) tend to have a more exacerbated anepectic behaviour than structures #2 Nylon-PVA #2 and #2 75%) as Figure 3.4 shows: Nylon- PVA #1 ($-520 \times 10^{-6}/^{\circ}C$), Nylon-PVA #1 75% ($-712 \times 10^{-6}/^{\circ}C$), Nylon-PVA #2 ($-230 \times 10^{-6}/^{\circ}C$) and Nylon-PVA #2 75% ($-292 \times 10^{-6}/^{\circ}C$). Besides, the data shown if Figure 3.4 is important to conclude that structures with less length (structures #1 75% compared with structures #1 and structures #2 75% compared with structures #2) tend to demonstrate more negative values of thermal expansion, regardless of their material combination, in which is possible to conclude that dual-material structures with lower length (structures #175% and #2 75%) are more desirable to obtain a more intense anepectic behaviour.

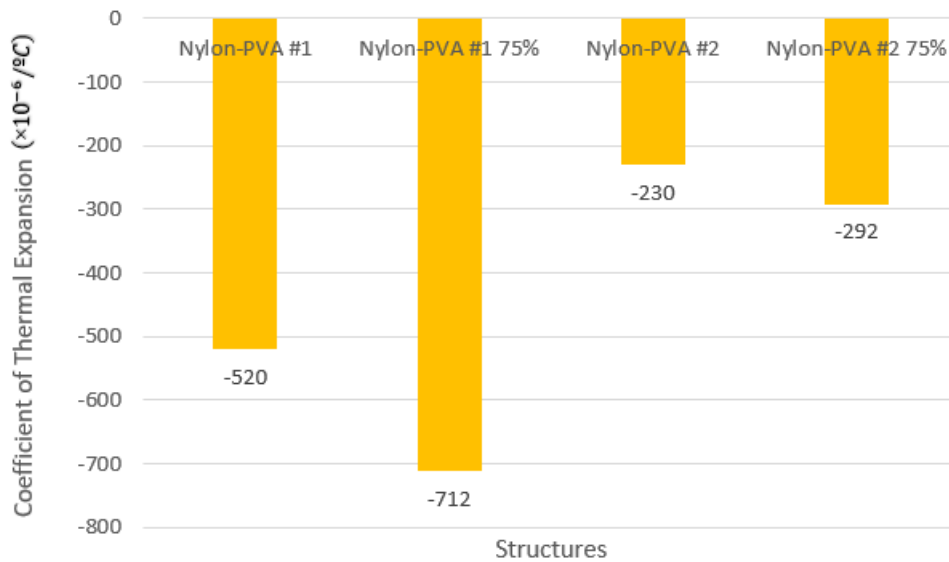


Figure 3.4 – CTE of structures #1, #1 75%, #2 and #2 75% in the material combination of Nylon-PVA at 80°C.

3.3.3 Effect of temperature above glass transition temperature

As already mentioned, anepectic behaviour only occurs when are used materials with similar (although different) stiffness but extremely different values of CTE and they must work above their Tg. Nylon-PVA samples were already subjected to an environment where temperature was above of the Tg of the polymers involved. However, at 80°C, Nylon-CPE+ sample does not work above the Tg of CPE+, as it can be seen in Table 3.3.

Table 3.3 – Values of Tg for Nylon, PVA and CPE+[1].

Material	Tg(°C)
Nylon	35
PVA	35
CPE+	105

In Figure 3.5, it is shown that three samples were taken into consideration: Nylon #1, Nylon-PVA #1 and Nylon-CPE+ #1. This experiment was done to clarify if, when both materials (Nylon and CPE+) undergo through temperatures above their T_g , the Nylon-CPE+ combination show anepctic behaviour, like the Nylon-PVA combination.

Figure 3.5 shows, as expected, that the single material structure (Nylon #1) has positive values of CTE, even when T_g is reached ($157 \times 10^6 / ^\circ\text{C}$ at 80°C and $129 \times 10^6 / ^\circ\text{C}$ at 120°C) and that the dual material Nylon-PVA structure shows anepctic behaviour only in temperatures above T_g ($-520 \times 10^6 / ^\circ\text{C}$ at 80°C and $-812 \times 10^6 / ^\circ\text{C}$ at 120°C). However, it is also possible to see that Nylon-CPE+ has always positive values of CTE, even when T_g is reached ($42 \times 10^6 / ^\circ\text{C}$ at 120°C). To sum up, Figure 3.5 shows that the Nylon-CPE+ combination isn't a good combination to obtain anepctic behaviour and, therefore, it doesn't deserve further investigation.

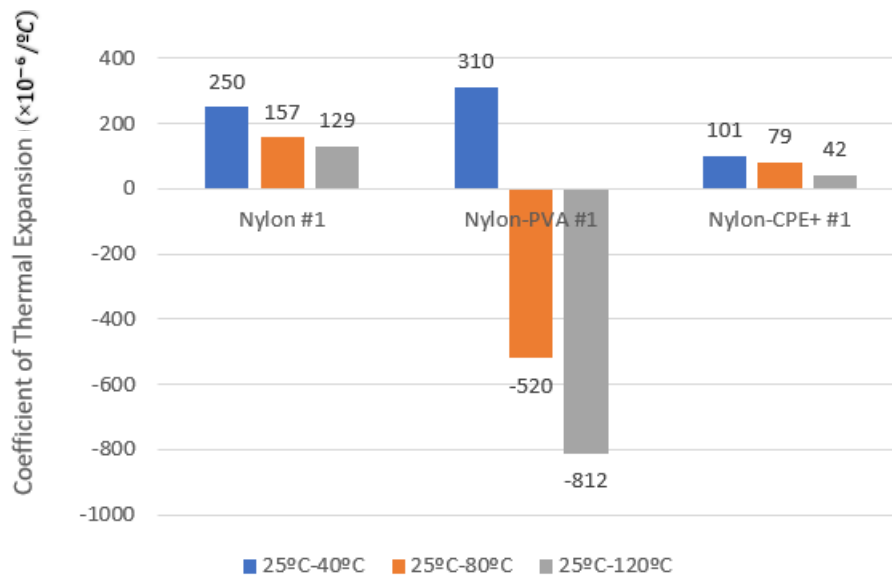


Figure 3.5 – CTE of structure #1 in different material combinations (Nylon, Nylon-PVA and Nylon-CPE+) at different ranges of temperature: 25°C to 40°C, 25°C to 80°C and 25°C to 120°C.

This work corroborates what was concluded by J. Raminhos *et al* [1]: samples composed by materials that have similar (although different) values of Young's Modulus and extremely different values of CTE, can exhibit anepctic behaviour only if they work above their respective T_g temperatures. Bearing in mind that the structures used in this work are familiar to the meshes studied in the paper by J. Raminhos *et al* [1], it can be seen that, in both cases, more complex samples exhibit less anepctic behaviour: half-scale meshes (compared with full-scale meshes) [1], thicker structures (comparing structures #1 with #1 75% and structures #2 with #2 75%) and structures with more complex geometry (comparing structures #2 with #1).

CONCLUSIONS AND FUTURE PERSPECTIVES

This thesis is an extension of the work developed by J. Raminhos *et al* [1], in which star-shaped re-entrant 3-D structures exhibiting anepectic behaviour – structures with the capability of exhibiting negative values of Poisson’s ratio and of CTE - were designed, printed and tested.

Two main structures were studied in this work. Structure #1 has four parameters - three length parameters (H1, H2 and t) and one angular parameter (θ). Structure #2 has five parameters - three length parameters (H1, H2 and t) and two angular parameters (θ and θ_o). The effect of those parameters on the structures’ behaviour were evaluated by thermo-mechanical tests. Both the structures demonstrate auxetic behaviour. However, structure #1 exhibits more negative values of Poisson’s ratio. The secondary structures (#1 75% and 2 75%) were useful to understand that thinner structures – lower values of the length parameter t -tend to exhibit a deeper auxetic behaviour.

As expected, anepectic behaviour could only be observed when the combined materials have similar (although different) stiffness but extremely different values of CTE. Besides, both the materials must be working above their respective Tg. The chosen materials to embody these structures are all polymers with positive values of CTE and of Poisson’s ratio, in which resulted in two material combinations: Nylon-PVA and Nylon-CPE+. In this work, anepectic behaviour could only be observed in the Nylon-PVA combination. This work proves experimentally that Nylon and CPE+ aren’t a good combination: their values of Young’s Modulus are too similar to tune negative values of CTE. In the Nylon-PVA structures, it was possible to conclude that structures #1 tend to have lower values of CTE compared with structures #2 and that structures with less length (#1 75% compared with #1 and #2 75% compared with #2) tend to contract more easily when heated, which means they exhibit a deeper anepectic behaviour.

Comparing this work with the paper by J. Raminhos *et al* [1], it can be seen that in both cases more complex samples exhibit less anepectic behaviour. However, this work managed to study the difference of length parameters (the paper by J. Raminhos *et al* [1] focuses on meshes whose length parameters - H1 and H2 - are equal). This work shows two types of length parameters (L1 and L2 for structures #1 and H1 and H2 for structures #2) in which the samples with less difference of length parameters (structures #1) exhibit a more exacerbated anepectic behaviour.

In a future perspective, further investigation about this topic (3-D anepectic structures) is required; it would be interesting to use other combinations of polymers. Considering that this work only focused on the variation of length (t), it would be interesting to investigate other parameters, such as the variation of angle (θ for structure #1; θ and θ_o for structure #2). Different values of H1 and H2 must also be studied. Besides, other types of structures (gyroid structure, e.g.) must be investigated. It is foreseeable that 3-D anepectic structures will be an asset in a great range of applications (biomedical field, electronics, aerospace and defence industry, e.g.), which gives further importance to the investigation required. Besides, considering that there’s investigation about 4-D auxetic structures [37], it would also be interesting if, in the next few years, a work about 4-D anepectic structures would come up to light. Thus, it would be possible to manufacture an anepectic structure that has the capability to change its configuration over time, due to an external stimulus.

REFERENCES

- [1] - J.S. Raminhos, A. Velhinho, J.P. Borges, “Development of Polymeric Anepectic Meshes: Auxetic Metamaterials with Negative Thermal Expansion”, *Smart Materials & Structures*, vol. 28, 045010, 2019. DOI: [10.1088/1361-665X/ab034b](https://doi.org/10.1088/1361-665X/ab034b)
- [2] - I. Marcelino, “Additive Fabrication of Anepectic Meshes controlled by a NiTi alloy”, M.Sc. thesis in Materials Engineering, Universidade Nova de Lisboa, 2019
- [3] – Yangbo Li, Yanyu Chen, Tiantian Li, Siyu Cao and Lifeng Wang, “Hoberman- Sphere-Inspired Lattice Metamaterials with Tunable Negative Thermal Expansion”, *Comp. Struct.*, vol. 189, no. 4, pp. 586-597, Apr. 2018. DOI: [10.1016/j.compstruct.2018.01.108](https://doi.org/10.1016/j.compstruct.2018.01.108)
- [4] - L. Wu, B. Li, and J. Zhou, “Isotropic Negative Thermal Expansion Metamaterials” *ACS Appl. Mater. Interfaces*, vol. 8, no. 27, pp. 17721–17727, Jul. 2016. DOI: [10.1021/acsami.6b05717](https://doi.org/10.1021/acsami.6b05717)
- [5] - Boatti E, Vasios N and Bertoldi K., “Origami Metamaterials for Tunable Thermal Expansion”, *Adv. Mater.*, vol. 29, no. 7, p. 1700360, Jul. 2017. DOI: [10.1002/adma.201700360](https://doi.org/10.1002/adma.201700360)
- [6] - Joseph N Grima, Pierre S Farrugia, Ruben Gatt and Victor Zammit, “A system with adjustable positive or negative thermal expansion”, *The Royal Soc. Pub.*, vol. 463, no. 3, pp. 1585- 1596, Marc. 2007. DOI: [10.1098/rspa.2007.1841](https://doi.org/10.1098/rspa.2007.1841)
- [7] - W. Miller, D.S. Mackenzie, C.W. Smith and K.E. Evans, “A generalised scale-independent mechanism for tailoring of thermal expansivity: Positive and negative”, *Mech. Mat.*, vol. 40, no. 4, pp. 351-361, Apr. 2008. DOI: [10.1016/j.mechmat.2007.09.004](https://doi.org/10.1016/j.mechmat.2007.09.004)
- [8] – K. Wei, H. Chen, Y. Pei, and D. Fang, “Planar lattices with tailorable coefficient of thermal expansion and high stiffness based on dual-material triangle unit” *J. Mech. Phys. Solids*, vol. 86, pp. 173–191, Jan. 2016. DOI: [10.1016/j.mechmat.2007.09.004](https://doi.org/10.1016/j.mechmat.2007.09.004)
- [9] - Jonathan B. Hopkins, Yuanping Song, Howon Lee, Nicholas X. Fang and Christopher M. Spadaccini, “Polytope Sector Based Synthesis and Analysis of Microstructural Architectures With Tunable Thermal Conductivity and Expansion”, *J. Mech. Design*, vol. 138, p. 051401, no. 5, May. 2016. DOI: [10.1115/1.4032809](https://doi.org/10.1115/1.4032809)
- [10] – Jingyuan Qu, Muamer Kadic, Andreas Naber and Martin Wegener, “Micro- Structured Two-Component 3D Metamaterials with Negative Thermal-Expansion Coefficient from Positive Constituents”, *Scient. Rep.*, vol. 7, no. 1, p. 40643, Jan. 2017. DOI: [10.1038/srep40643](https://doi.org/10.1038/srep40643)
- [11] – Mozafar Shokri Rad, Yunan Prawoto and Zaini Ahmad, “Analytical Solution and finite element approach to the 3D re-entrant structures of auxetic materials”, *Mech. of Mat.*, vol. 74, no. 7, pp. 76-87, Jul. 2014. DOI: [10.1016/j.mechmat.2014.03.012](https://doi.org/10.1016/j.mechmat.2014.03.012)
- [12] - C. Huang and L. Chen, “Negative Poisson’s Ratio in Modern Functional Materials”, *Adv. Mater.*, vol. 28, no. 37, pp. 8079–8096, Oct. 2016. DOI: [10.1002/adma.201601363](https://doi.org/10.1002/adma.201601363)
- [13] - J. Parada, “Additive fabrication of electrically controlled anepectic meshes”, M.Sc. thesis in Materials Engineering, Universidade Nova de Lisboa, 2019
- [14] - K. E. Evans, M. A. Nkansah, I. J. Hutchinson, and S. C. Rogers, “Molecular network design”, *Nature*, vol. 353, p. 124, Sep. 1991. DOI: [10.1038/353124a0](https://doi.org/10.1038/353124a0)
- [15] - R. Lakes, “Foam Structures with a Negative Poisson’s Ratio”, *Science*, vol. 235, no. 4792, pp. 1038–1040, Feb. 1987. DOI: [10.1126/science.235.4792.1038](https://doi.org/10.1126/science.235.4792.1038)

- [16] - A. E. H. Love, “A Treatise on the Mathematical Theory of Elasticity”, Dover, New York, 1944. DOI: [10.1016/j.commatsci.2012.02.012](https://doi.org/10.1016/j.commatsci.2012.02.012)
- [17] - Yunan Prawoto, “Seeing Auxetic Materials from the mechanics point of view: A structural review on the negative Poisson’s Ratio”, *Comp. Mat. Science*, vol. 58, no. 6, pp. 140-152, Jun. 2012. DOI: [10.1016/j.commatsci.2012.02.012](https://doi.org/10.1016/j.commatsci.2012.02.012)
- [18] - Małgorzata Janus-Michalska, “Micromechanical Model of Auxetic Cellular Materials”, *J. of Theor. and Appl. Mech.*, vol. 47, no. 4, pp. 737-750, Apr. 2009. DOI: [10.1126/science.235.4792.1038](https://doi.org/10.1126/science.235.4792.1038)
- [19] - João Valente, Eric Plum, Ian J. Youngs, Nikolay I. Zheludev, “Nano- and Micro-Auxetic Plasmonic Materials”, *Adv. Mat.*, vol. 28, no. 5, pp. 5176-5180, May. 2016. DOI: [10.1002/adma.201600088](https://doi.org/10.1002/adma.201600088)
- [20] - Roderic S. Lakes, “Polyhedron cell structure and method of making same”, University of Iowa Patents, US Patent 4,668,557, May. 1987. DOI: [10.1073/pnas.1509663112](https://doi.org/10.1073/pnas.1509663112)
- [21] - M. H. Fu, O. T. Xu, L. L. Hu, and T. X. Yu, “Nonlinear shear modulus of re-entrant hexagonal honeycombs under large deformation”, *Int. J. Solids Struct.*, vol. 80, pp. 284– 296, Feb. 2016. DOI: [10.1016/j.ijsolstr.2015.11.015](https://doi.org/10.1016/j.ijsolstr.2015.11.015)
- [22] - C. Huang and L. Chen, “Negative Poisson’s Ratio in Modern Functional Materials”, *Adv. Mater.*, vol. 28, no. 37, pp. 8079–8096, Oct. 2016. DOI: [10.1002/adma.201601363](https://doi.org/10.1002/adma.201601363)
- [23] – Krishna Kumar Saxena, “Three Decades of Auxetics Research – Materials with Negative Poisson’s Ratio: A Review”, *Adv. Eng. Mat.*, vol. 18, no. 11, pp. 1847-1870, Nov. 2016. DOI: [10.1002/adem.201600053](https://doi.org/10.1002/adem.201600053)
- [24] - X.-T. Wang, B. Wang, X.-W. Li, and L. Ma, “Mechanical properties of 3D re-entrant auxetic cellular structures” *Int. J. Mech. Sci.*, vol. 131–132, no. March, pp. 396–407, Oct. 2017. DOI: [10.1016/j.ijmecsci.2017.05.048](https://doi.org/10.1016/j.ijmecsci.2017.05.048)
- [25] - R. Lakes, Roderic SLakes, “Negative-Poisson’s-Ratio Materials: Auxetic Solids”, *Annu. Rev. Mater. Res.*, vol. 47, no. 1, pp. 63–81, Jul. 2017. DOI: [10.1146/annurev-matsci-070616-124118](https://doi.org/10.1146/annurev-matsci-070616-124118)
- [26] - M. Shokri Rad, Y. Prawoto, and Z. Ahmad, “Analytical solution and finite element approach to the 3D re-entrant structures of auxetic materials”, *Mech. Mater.*, vol. 74, no. 7, pp. 76–87, Jul. 2014. DOI: [10.1016/j.mechmat.2014.03.012](https://doi.org/10.1016/j.mechmat.2014.03.012)
- [27] – K. L. Alderson, K. E. Evans, “The fabrication of microporous polyethylene having a negative Poisson ’s ratio”, *Polymer*, vol. 33, no. 20, pp. 4435-4438, 1992. DOI: [10.1016/0032-3861\(92\)90294-7](https://doi.org/10.1016/0032-3861(92)90294-7)
- [28] - Dennis M Kochmann and Gabriela N Venturini, “Homogenized mechanical properties of auxetic composite materials in finite-strain elasticity”, *Smart Mat. And Struc.*, vol. 22, no. 8, Jul. 2013. DOI: [10.1088/0964-1726/22/8/084004](https://doi.org/10.1088/0964-1726/22/8/084004)
- [29] - Luke Mizzi, Daphne Attard, Aaron Casha and Joseph N. Grima, “On the suitability of hexagonal honeycombs as stent geometries”, *Phis. Stat. Sol.*, vol. 251, no. 2, pp. 328-337, Fev. 2014. DOI: [10.1002/pssb.201384255](https://doi.org/10.1002/pssb.201384255)
- [30] – Davood Mousanezhad, Sahab Babae, Hamid Ebrahimi, Ranajay Ghosh, Abdelmagid Salem Hamouda, Katia Bertoldi and Ashkan Vaziri, “Hierarchical honeycomb auxetic metamaterials”, *Scient. Rep.*, vol. 5, p. 18306, 2015. DOI: [10.1038/srep18306](https://doi.org/10.1038/srep18306)

- [31] – J. N. Grima, R. Gatt, A. Alderson and K. E. Evans, “On the potential of connected stars as auxetic systems”, *Molec. Simul.*, vol. 31, no. 13, pp. 925-935, Nov. 2006. DOI: [10.1080/08927020500401139](https://doi.org/10.1080/08927020500401139)
- [32] – A. Spadoni and M. Ruzzene, “Elasto-static micropolar behaviour of a chiral auxetic lattice”, *J. of the Mech. and Phys. of Sol.*, vol. 60, no. 1, pp. 156-171, Jan. 2012. DOI: [10.1016/j.jmps.2011.09.012](https://doi.org/10.1016/j.jmps.2011.09.012)
- [33] – J. N. Grima, V. Zammit, R. Gatt, A. Alderson and K.E. Evans, “Auxetic behaviour from rotating semi-rigid units”, vol. 244, no. 3, pp. 866-882, Mar. 2007. DOI: [10.1002/pssb.200572706](https://doi.org/10.1002/pssb.200572706)
- [34] – Shangqin Yuan, Fei Shen, Jiaming Bai, Chee Kai Chua, Jun Weiu and Kunzhou, “3D soft auxetic lattice structures fabricated by selective laser sintering: TPU powder evaluation and process optimization”, *Mat. and Des.*, vol. 120, no. 4, pp. 317-327, Apr. 2017. DOI: [10.1016/j.matdes.2017.01.098](https://doi.org/10.1016/j.matdes.2017.01.098)
- [35] – Eric B. Duoss, Todd H. Weisgraber, Keith Hearon, Cheng Zhu, Ward Small IV, Thomas R. Metz, John J. Vericella, Holly D. Barth, Joshua D. Kuntz, Robert S. Maxwell, Christopher M. Spadaccini and Thomas S. Wilson, “Three-dimensional printing of elastomeric, cellular architectures with negative stiffness”, *Adv. Funct. Mat.*, vol. 24, no. 8, pp. 4905-49134, Aug. 2014. DOI: [10.1002/adfm.201400451](https://doi.org/10.1002/adfm.201400451)
- [36] – Li Yang, Ola Harrison, Harvey West and Denis Cormier, “Mechanical properties of 3D re-entrant honeycomb auxetic structures realized via additive manufacturing”, *Int. Journ. Of Sold. and Struc.*, vo. 69, no. 9, pp. 475-490, Sep. 2015. DOI: [10.1016/j.ijsolstr.2015.05.005](https://doi.org/10.1016/j.ijsolstr.2015.05.005)
- [37] – S. Pandini, N. Inverardi, G. Scalet, *et al*, “Shape memory response and hierarchical motion capabilities of 4D printed auxetic structures”, *Mech. Res. Commun.*, vol. 103, no.1, Jan.2020. DOI: [10.1016/j.mechrescom.2019.103463](https://doi.org/10.1016/j.mechrescom.2019.103463)
- [38] - Simon Meteyer, Xin Xu, Nicolas Perry, Yaoyao Fiona Zhao, “Energy and Material Flow Analysis of Binder-jetting Additive Manufacturing Processes”, *Procedia CIRP*, vol. 15, no. 6, pp. 19-25, Jun. 2014. DOI: [10.1016/j.procir.2014.06.030](https://doi.org/10.1016/j.procir.2014.06.030)
- [39]– Brian N. Turner, Robert Strong, Scott A. Gold, “A review of melt extrusion additive manufacturing processes: I. Process design and modelling”, *Rapid Prototip. J.*, vol. 20, no. 3, pp. 192-204, Apr. 2014. DOI: [10.1108/RPJ-01-2013-0012](https://doi.org/10.1108/RPJ-01-2013-0012)
- [40]- Mohd. Javaid and Abid Haleem, “Additive Manufacturing Applications in medical cases: A literature based review”, *Alexandria J. of Med.*, vol. 54, no. 4, pp. 411-422, May. 2019. DOI: [10.1016/j.ajme.2017.09.003](https://doi.org/10.1016/j.ajme.2017.09.003)
- [41]– Alessandro Busachi, John Erkoyuncu, Paul Colegrove, Richard Drake, Chris Watts and Filomeno Martina, “Defining Next-Generation Additive Manufacturing Applications for the Ministry of Defence (MoD)”, *Procedia CIRP*, vol. 55, pp. 302-307, 2016. DOI: [10.1016/j.procir.2016.08.029](https://doi.org/10.1016/j.procir.2016.08.029)
- [42] – R. Liu, Z. Wang, T. Sparks, F. Liou and J. Newkirk, “Aerospace applications of laser additive manufacturing”, *Laser Add. Manuf.*, pp. 351-371, 2017. DOI: [10.1016/B978-0-08-100433-3.00013-0](https://doi.org/10.1016/B978-0-08-100433-3.00013-0)
- [43] - J. N. Grima, P.S. Farrugia, R. Gatt, and V. Zammit, “Connected Triangles Exhibiting Negative Poisson’s Ratios and Negative Thermal Expansion”, *J. Phys. Soc. Japan*, vol. 76, no. 2, p. 025001, Feb. 2007. DOI: [10.1143/JPSJ.76.025001](https://doi.org/10.1143/JPSJ.76.025001)

[44] - L. Ai and X. Gao, “Metamaterials with negative Poisson ’s ratio and non-positive thermal expansion”, *Compos. Struct.*, vol. 162, pp. 70–84, 2017. DOI: [10.1016/j.compstruct.2016.11.056](https://doi.org/10.1016/j.compstruct.2016.11.056)

[45] - L. Ai and X. L. Gao, “Three-dimensional metamaterials with a negative Poisson’s ratio and a non-positive coefficient of thermal expansion”, *Int. J. Mech. Sci.*, vol. 135, no. September 2017, pp. 101–113, 2018. DOI: [10.1016/j.ijmecsci.2017.10.042](https://doi.org/10.1016/j.ijmecsci.2017.10.042)

[46] - Mozafar Shokri Rad, Yunan Prawoto and Zaini Ahmad, “Computational Approach in Formulating Mechanical Characteristics of 3D Star Honeycomb Auxetic Structure”, *Adv. in Mat. Sc. and Eng.*, vol.2015, no 1,Jan.2015. DOI: [10.1155/2015/650769](https://doi.org/10.1155/2015/650769)

APPENDIX

APPENDIX A – REPRESENTATIVE SCHEME AND DESCRIPTION OF THE TESTING STRUCTURE

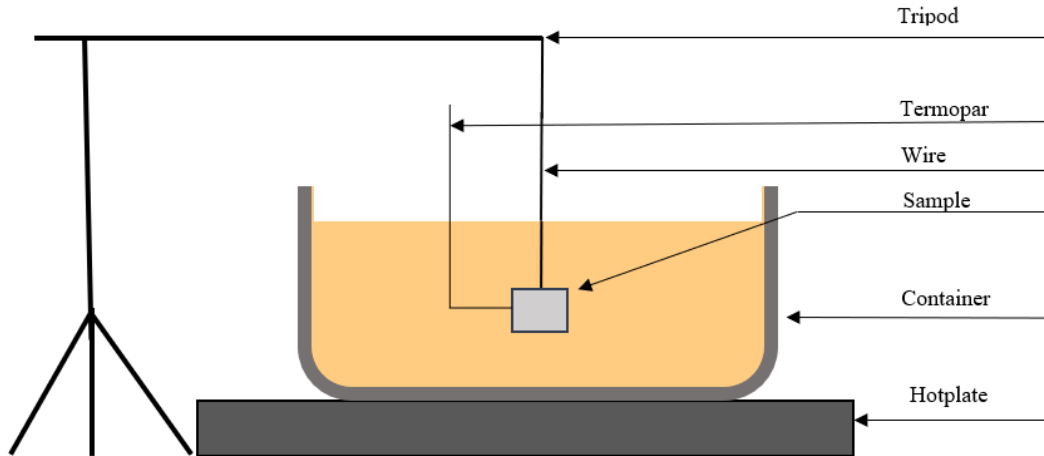


Figure A.1 – Representative scheme and description of the testing structure performed in this work.

APPENDIX B – EQUATIONS FOR THE CALCULATION OF PR AND CTE

To calculate the values of the Poisson's ratio the following equation was considered:

$$\nu_{yz} = -\frac{\ln\left(1+\frac{\Delta y}{y_0}\right)}{\ln\left(1+\frac{\Delta z}{z_0}\right)} \text{ (Equation B.1)}$$

In which Δz refers to the elongation in the transverse direction, z_0 corresponds to the original length in the transverse direction, Δy represents the elongation in the axial direction and y_0 means the original length in the axial direction.

The values of CTE were calculated considering the following equation:

$$\alpha = \frac{\Delta l}{l_0} \times \frac{1}{\Delta T} \text{ (Equation B.2)}$$

In which ΔT corresponds to thermal variation, Δl refers to length variation and l_0 represents the initial length.

APPENDIX C – TENSILE CURVES OF THREE POLIMERIC MATERIALS

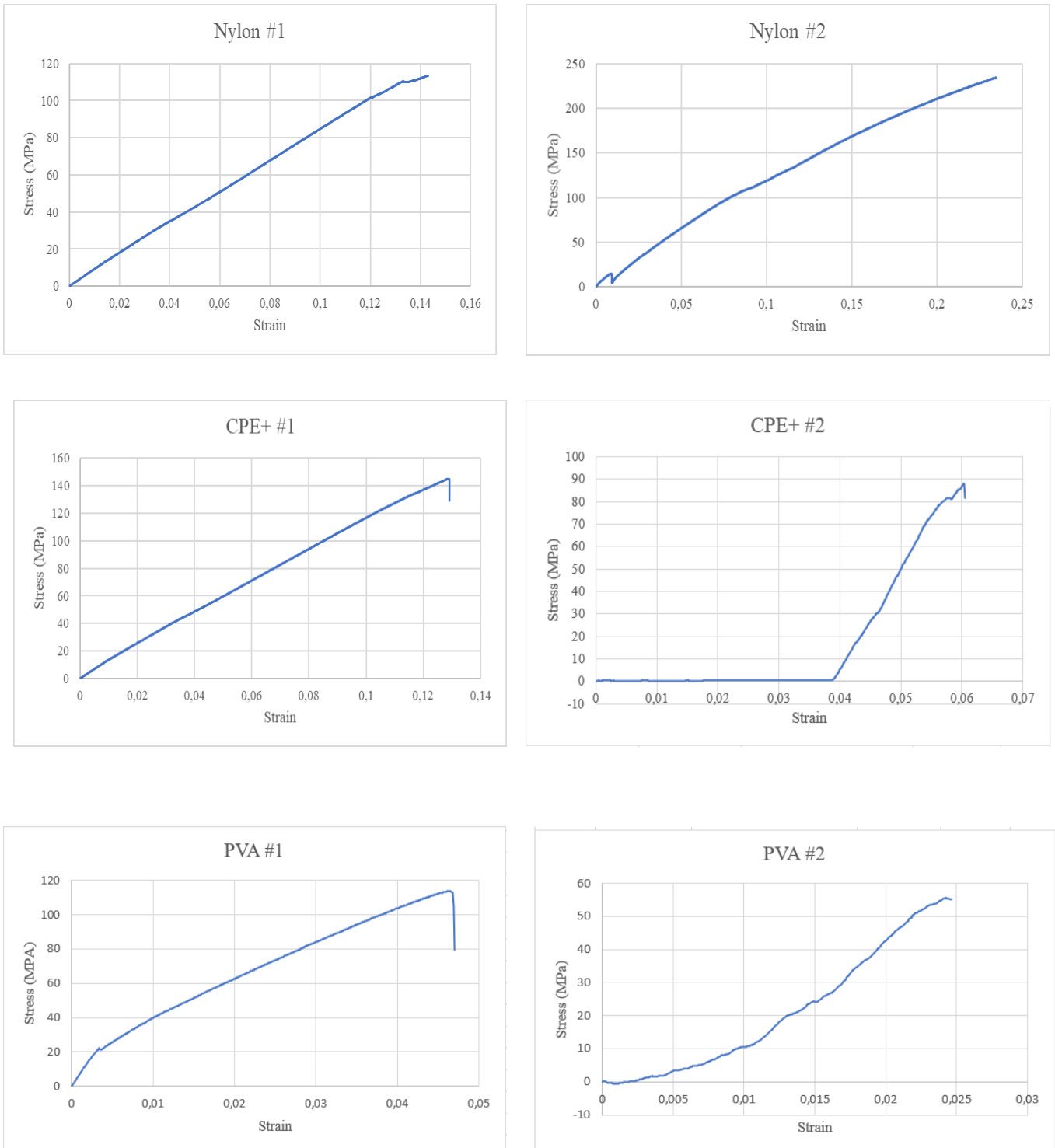


Figure C.1 - Tensile curves of three polymeric materials (Nylon, CPE+ and PVA) used in this work as constituents of the printed structures. The materials used were commercially available Ultimaker™ filaments. The specimens were tractioned (2 mm/min) by using a universal testing machine (AG-50kNG, Shimadzu, Japan).

APPENDIX D – MATERIALS' PROPERTIES USED IN THIS WORK

Table D.1 - The materials' properties used in this work. All the polymers used are commercially available Ultimaker™ filaments and they were tested to determine their values of CTE and of Young's Modulus. These values are important to determine which are the best combinations to obtain an anepectic behaviour.

Materials	Young's Modulus (MPa)
Nylon #1	0.817
Nylon #2	0.996
CPE+ #1	1.129
CPE+ #2	1.269
PVA #1	2.224
PVA #2	2.506

Structures	CTE ($\times 10^6/^\circ\text{C}$)
Nylon #1	157
Nylon #1 75%	178
Nylon #2	126
Nylon #2 75%	134
CPE+ #1	70
CPE+ #2	46
PVA #1	19
PVA #2	14

APPENDIX E – CTE MEASURING PROCEDURE:

Circles are painted on the analysed structure in different places, as indicated in Figure E.1. Two temperatures were considered: T_i and T_f . Two different positions were considered - A and B - both represented in Figure E.1. The following steps were taken:

1. Measure the x and y coordinates of A and B positions at T_i and T_f .
2. Measure the distance between the A and B at T_i , with the formula:

$$dT_i = \sqrt{(x_{AT_i} - x_{BT_i})^2 + (y_{AT_i} - y_{BT_i})^2} \quad (\text{Equation E.1})$$

3. Measure the distance between A and B at T_f , with the following formula:

$$dT_f = \sqrt{(x_{AT_f} - x_{BT_f})^2 + (y_{AT_f} - y_{BT_f})^2} \quad (\text{Equation E.2})$$

4. Measure the shrinkage between dT_i and dT_f :

$$\text{Shrinkage (\%)} = \frac{dT_f - dT_i}{T_f - T_i} \quad (\text{Equation E.3})$$

5. Measure the values of CTE:

$$\text{CTE} = \frac{\text{Shrinkage (\%)}}{T_f - T_i} \quad (\text{Equation E.4})$$

6. After calculating the CTE values for all the fixed points in the sample, an average is made to obtain the final value of CTE.

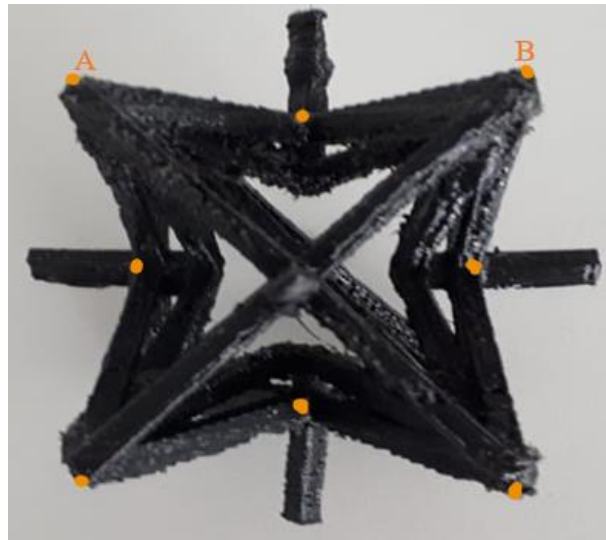


Figure E.1 – Sample Nylon #2 with the circles marked, and the A and B representative positions.

APPENDIX F – POISSON'S RATIO MEASURING PROCEDURE:

1. Four points are taken as reference (P1, P2, P3 and P4) in the non-deformed structure, as it can be seen in Figure F.1.
2. Equidistant points of reference are taken (PmiA, PmiB.), according to the coordinated direction (i=x,y,z).
3. Distantce between the equidistant points are measured (wx, wy, wz).
4. After tensile tests, four points are taken as reference (P1', P2'; P3' and P4') in the deformed structure.
5. Equidistant points of reference are taken (P'MiA, P'miB), according to the coordinated direction (i=x,y,z).
6. Distantce between the equidistant points are measured (w'x, w'y and w'z). It's important to note that:

$$w'x = wx + \Delta wx; \quad w'y = wy + \Delta wy; \quad w'z = wz + \Delta wz \quad (\text{Equations F.1, F.2 and F.3})$$

In which Δwx , Δwy and Δwz correspond to the distance variation between equidistant points after deformation.

7. Finally, Poisson's ratio can be calculated:

$$v_{yz} = -\frac{\ln\left(1+\frac{\Delta wy}{wy}\right)}{\ln\left(1+\frac{\Delta wz}{wz}\right)}; \quad v_{xz} = -\frac{\ln\left(1+\frac{\Delta wx}{wx}\right)}{\ln\left(1+\frac{\Delta wz}{wz}\right)} \quad (\text{Equations F.4, F.5})$$

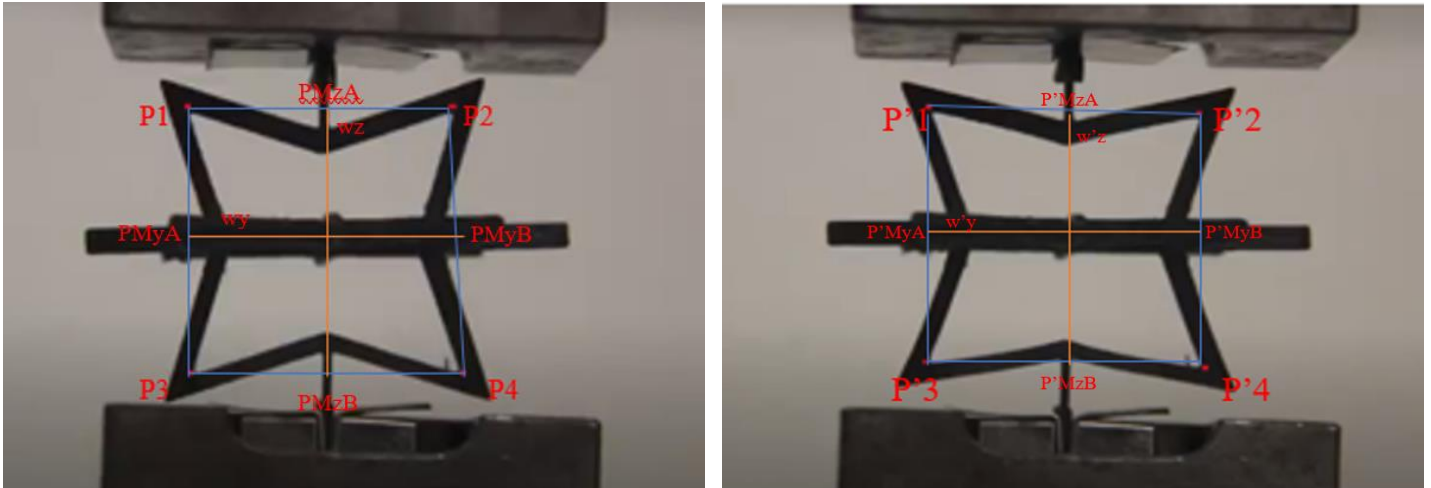


Figure F.1 – Sample Nylon #2 during tensile tests: a) – Sample Nylon #1 non-deformed; b) – Sample Nylon #1 deformed.